



# Magnetic horsetail plant ash ( $\text{Fe}_3\text{O}_4@HA$ ): a novel, natural and highly efficient heterogeneous nanocatalyst for the green synthesis of 2,4,5-trisubstituted imidazoles

Nina Hosseini Mohtasham<sup>1</sup> · Mostafa Gholizadeh<sup>1</sup>

Received: 2 December 2020 / Accepted: 27 February 2021  
© The Author(s), under exclusive licence to Springer Nature B.V. 2021

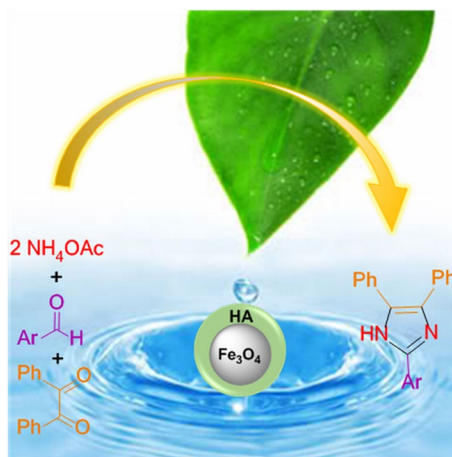
## Abstract

Horsetail plant ash (HA), as a natural source of mesoporous silica, has been prepared from the exposure of horsetail plant (*Equisetum Arvense*) to high temperature. In the present study, a new magnetically separable and also recoverable  $\text{Fe}_3\text{O}_4$  nanoparticles were synthesized in the presence of natural horsetail plant ash (HA) as a support to result in  $\text{Fe}_3\text{O}_4@HA$ . FT-IR, XRD, TEM, SEM–EDX and VSM analysis were combined to characterize the morphology and structure of this novel synthesized nanocatalyst. This magnetically solid acid nanocatalyst showed an excellent catalytic activity for the synthesis of 2,4,5-trisubstituted imidazoles at room temperature in aqueous media. The procedure led to corresponding products in high to excellent yields and appropriate times. Additionally, this nanocatalyst can be easily recovered by a magnetic field and reused for six other consecutive reaction runs without noticeable loss of its catalytic efficiency. Based on this study,  $\text{Fe}_3\text{O}_4@HA$  is found to be an efficient, magnetically separable, recyclable, and green catalyst with natural source.

## Graphic abstract

In this work, horsetail plant ash was used as a natural source of mesoporous silica for the synthesis of  $\text{Fe}_3\text{O}_4@HA$  as a highly powerful magnetically solid acid nanocatalyst, which was fully characterized using various techniques. The activity of the

newly synthesized nanocatalyst was tested for the synthesis of 2,4,5-trisubstituted imidazole derivatives.



**Keywords** Horsetail ash · Nano magnetic catalyst · 2,4,5-Trisubstituted imidazoles · One-pot reaction

## Introduction

Green chemistry principles are believed to be one of the effective and prevalent factors in today's organic synthetic protocols which are primarily concerned with alternative reaction media [1]. Having undergone commercial development, these media have become the basis of many of the cleaner chemical technologies. Green chemistry is mainly aimed to develop process selectivity, enlarge the use of starting materials, as well as replacing hazardous and stoichiometric reagents with eco-friendly catalysts in order to expedite the easy separation of final reaction mixtures, such as catalyst recovery [2–4].

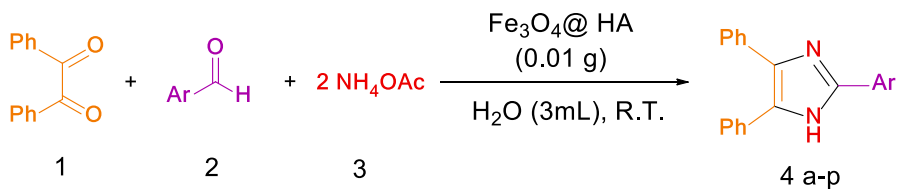
Due to numerous efficient factors including magnetic and electrical properties, high specific surface area, unique catalytic and wide applications in drug delivery systems, targeted gene therapy, ion exchange separation, magnetic resonance imaging, biosensors, magnetic data storage, and environmental remediation and catalysis [5–7], magnetic nanoparticles (MNPs) such as magnetite (Fe<sub>3</sub>O<sub>4</sub>) have attracted great interest among practitioners in green chemistry. It is worth noting that the insoluble and paramagnetic nature of Fe<sub>3</sub>O<sub>4</sub> enables trouble-free separation of this nanocatalyst from the reaction mixture by applying an external magnet eliminating the necessity of catalyst filtration which prevents loss of the catalyst. Recent scholars, accordingly, have acquired immense and valuable interests within the synthesis and application of magnetically recoverable catalysts as a fascinating choice to increase the efficiency of heterogeneous nanocatalyst

separation from the reaction mixture by simply utilizing a magnet [8]. Magnetite nanoparticles are suitable to be chemically stable and uniform in size; however, they tend to aggregate due to their nanoscale and strong interaction among each other. Hopefully, this problem can be overcome by their coating with a layer as the stabilizer, leading to the prevention of direct contacts among the nanoparticles in addition to enhancing the stability of them [9–12].

In our earlier research, horsetail and horsetail ash as novel, inexpensive and available heterogeneous natural mild solid acid catalysts as well as their interesting properties and catalytic activities were completely discussed and investigated [13]. It was further recommended that the horsetail ash could be used as support for the preparation of a variety types of catalysts due to its high surface area and high silica content that could serve as a natural silica resource having mesoporous structure.

Throughout this century, Imidazole functional group and more particularly 2,4,5-trisubstituted imidazoles have received significant attention in organic synthesis and have found many applications as a result of their biological and pharmacological activities [14–20]. Imidazoles which are the core fragment of different natural products such as histamine, histidine, biotin, alkaloids, peptides, and nucleic acids are classified as an important class of heterocycles [21]. The recently developed green chemistry and organometallic chemistry have increased the utility and efficacy of imidazoles as green solvents in terms of ionic liquids [22–24] and as N-heterocyclic carbenes [25, 26]. Also, it must be noted that in the recent past, the synthesis of imidazole and its derivative has drawn much attention owing to their wide range of pharmacological activity in addition to their industrial and synthetic applications. A considerable number of methods and procedures have been reported in the research literature for the one-pot synthesis of 2,4,5-trisubstituted imidazoles by cyclocondensation of benzil, aromatic aldehyde and ammonium acetate, under distinct condition [27–43]

It is a widely held view that all reported methods have their own merits, yet most of them are closely associated with one or more shortcomings and weaknesses such as use of carcinogenic organic solvents, application of high temperatures, harsh and tough reaction conditions, poor yield and production, use of expensive and toxic catalysts, lack of catalyst reusability, consumption of large amounts of catalyst, and long-lasting reaction time. Consequently, due to the fact that imidazoles are considered to have pharmaceutical significance, the establishment of new catalytic systems in order to overcome these drawbacks and enable simple, mild, green, and economical synthesis of imidazole derivatives would be highly beneficial and advisable. In regard to the preceding discussion, one of the remarkable highlights of the current paper is to introduce horsetail plant ash as a source of silica and use it as a support on the surface of  $\text{Fe}_3\text{O}_4$  which is present in one nano-structure ( $\text{Fe}_3\text{O}_4\text{@HA}$ ). In this research, the magnetic horsetail plant ash has been used for the first time to act as a recoverable catalytic system for the synthesis of trisubstituted imidazoles by one-pot three-component reaction of benzil, various aromatic aldehydes and ammonium acetate under aqueous conditions (Scheme 1).



**Scheme 1** Synthesis of trisubstituted imidazoles using  $\text{Fe}_3\text{O}_4@ \text{HA}$  as a green and recoverable nanomagnetic catalyst

## Experimental section

### Materials and instruments

All chemical materials and solvents were purchased from Sigma-Aldrich and Merck companies and were used without further purification. Subsequently, the products were characterized through the comparison of their physical data, IR,  $^1\text{H}$  NMR, and  $^{13}\text{C}$  NMR spectra with known samples. The progress of the reaction was monitored via thin layer chromatography (TLC) applying aluminum plates coated with silica gel polygram STL G/UV 254 (Merck) using n-hexane and ethyl acetate as eluents. The melting points were evaluated by an electrothermal type 9100 melting point apparatus. Mass analysis was performed by Agilent technology (HP) 5973, mass spectrometer functioning at an ionization potential of 70 eV. The  $^1\text{H}$  NMR and  $^{13}\text{C}$  NMR spectra were recorded on a Bruker Avance, at 300 and 75 MHz, respectively, utilizing TMS as an internal standard and  $\text{DMSO}-d_6$  as the solvent. The Fourier transform infrared (FT-IR) spectra were recorded from KBr disk within the region range of 400 to  $4000 \text{ cm}^{-1}$  utilizing an AVATAR 370 FT-IR Thermo Nicolet spectrometer. Crystallinity and textural patterns of the catalyst were investigated by XRD analysis applying a Panalytical company X'Pert Pro MPD diffractometer with Cu Ka ( $\lambda = 0.154 \text{ nm}$ ) X-ray irradiation source in a  $2\theta$  range between  $10^\circ$  and  $80^\circ$ . A transmission electron microscope (TEM) analysis was performed on a Leo 912 AB microscope (Zeiss, Germany) at an accelerating voltage of 120 kV. Scanning electron microscopy (SEM) images and energy-dispersive X-ray spectroscopy (EDX) results were obtained from Leo1450 VP operated at an accelerating voltage of 20 kV. The magnetic property of catalyst was examined by a vibrating sample magnetometer (VSM) technique in 1.5 T external magnetic fields at room temperature using magnetic Danesh pajoh instrument. All yields refer to isolated products after being purified by recrystallization.

### Preparation of magnetic horsetail plant ash ( $\text{Fe}_3\text{O}_4@ \text{HA}$ )

As stated in the preparation stage of our earlier research [13], in the initial phase horsetail plant was purchased from the market, washed several times to remove any adhering materials and then dried at room temperature for 24 h. Afterward, the dried plant was smashed and sieved (80-mesh size) and again washed and dried at  $110^\circ \text{C}$

for 5 h. Accordingly, mesoporous horsetail ash was prepared by thermal processing of the horsetail at  $400\text{ }^\circ\text{C}$  for 12 h. Following this,  $\text{Fe}_3\text{O}_4\text{@HA}$  was synthesized by adding  $\text{FeCl}_3\cdot 6\text{H}_2\text{O}$  (5 g) and  $\text{FeCl}_2\cdot 4\text{H}_2\text{O}$  (2 g) to a suspension of horsetail ash (1 g) in 60 mL of deionized water in a beaker. Afterward, we let the mixture stir strongly at  $80\text{ }^\circ\text{C}$  in order to obtain a clear solution, and then aqueous ammonia was dropped very slowly into the mixture until the pH of 12 was obtained. The resulting black solution was kept at  $80\text{ }^\circ\text{C}$  under vigorous stirring for further 30 min. At a later stage, the obtained magnetic nanoparticles were separated from solution by a powerful magnet and were washed repeatedly for three times with deionized water and eventually dried in vacuum at  $60\text{ }^\circ\text{C}$  for 8 h to result in a novel nanocatalyst. Throughout the synthesis, horsetail ash acted as a stabilizer and after the synthesis,  $\text{Fe}_3\text{O}_4$  nanoparticles were functionalized by horsetail ash (Scheme 2).

### General procedure for the synthesis of 2,4,5-trisubstituted imidazoles

$\text{Fe}_3\text{O}_4\text{@HA}$  (10 mg) was added to a mixture of benzil 1 (1 mmol), various aromatic aldehydes 2 (1 mmol) and ammonium acetate 3 (2 mmol) in 3 mL  $\text{H}_2\text{O}$  and was stirred at room temperature in an appropriate time as reported in Table 2. Later, when the reaction was completed (monitored and checked by TLC: n-hexane/ ethyl acetate, 7/3), water was removed from the reaction mixture under reduced pressure, and in the following step, the reaction mixture was dissolved in hot ethanol (5 mL) and the catalyst was removed magnetically by means of an external magnet and then it was washed with ethanol and dried to use it in other reactions. Thereafter, the reaction mixture was allowed to get cool at room temperature to recrystallize from ethanol to yield the pure final product. All the compounds were recognized and confirmed on the basis of their melting points as well as being compared with those reported in the literature and also via the spectroscopic method using FT-IR, Mass,  $^1\text{H}$  and,  $^{13}\text{C}$  NMR.

## Results and discussion

### Characterization of catalyst

Based on the method shown in Scheme 2, the modification of  $\text{Fe}_3\text{O}_4$  NPs with horsetail ash as a source of silica was acquired resulting in the preparation of  $\text{Fe}_3\text{O}_4\text{@HA}$



**Scheme 2** General route towards the synthesis of  $\text{Fe}_3\text{O}_4\text{@HA}$

as a novel solid acid magnetic nanocatalyst. Both the successful construction and the structure of this synthesized nanocatalyst were fully identified and verified by using various spectroscopic and microscopic techniques including Fourier transform infrared (FT-IR) spectroscopy, X-ray diffraction analysis (XRD), transmission electron microscopy (TEM), scanning electron microscopy (SEM) images, energy-dispersive X-ray spectroscopy (EDX), and vibrating sample magnetometer (VSM). The FT-IR spectra of a) horsetail plant, b) horsetail plant ash, c) magnetic horsetail plant ash and d) 6th reused  $\text{Fe}_3\text{O}_4\text{@HA}$  are illustrated in Fig. 1. As indicated in the FT-IR spectrum of horsetail plant (Fig. 1a), the most typical and standard broad band in the region from  $3500$  to  $3300\text{ cm}^{-1}$  comes from O–H stretching vibrations of silanol OH groups and the H–O–H vibration of water molecule adsorbed on the silica surface [44]. In addition, the distinctive bands at  $2923$  and  $2851\text{ cm}^{-1}$  are related to the asymmetric and symmetric methylene C–H stretching vibrational frequencies from aliphatic saturated compounds, respectively [45]. A weak peak around  $1734\text{ cm}^{-1}$  was determined to be associated to the C=O stretching of the related organic compounds [46]. Moreover, the absorption band at  $1636\text{ cm}^{-1}$  was attributed to the bending vibrational modes of the surface-attached hydroxyl groups (Si–OH) [47]. The sharp peak at  $1100\text{ cm}^{-1}$  could be referred to the Si–O–Si asymmetric stretching vibration, while the characteristic bands at  $813$  and  $468\text{ cm}^{-1}$  were allocated to the symmetric and bending vibration of Si–O–Si bond, respectively [48]. A closer look at Fig. 1a, b reveals significant changes in FT-IR spectra. As illustrated in Fig. 1b, the horsetail ash is acquired through the exposure of horsetail plant to high temperature resulting in the removal of all organic group peaks. In contrast to the curve shown in Fig. 1b, a new strong peak appeared at around  $578\text{ cm}^{-1}$  in Fig. 1c that

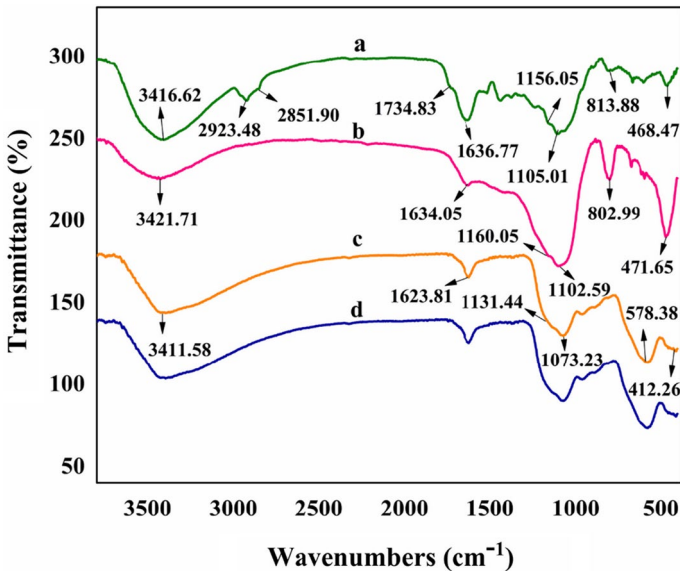


**Fig. 1** FT-IR spectra of (a) Horsetail plant, (b) Horsetail plant ash, (c) Magnetic horsetail plant ash ( $\text{Fe}_3\text{O}_4\text{@HA}$ ), and (d) 6th reused  $\text{Fe}_3\text{O}_4\text{@HA}$

can be ascribed to the vibration of Fe–O bonds confirming the  $\text{Fe}_3\text{O}_4$  phase, which is consistent to XRD analysis [49]. As demonstrated in Fig. 1c, the encapsulation of the  $\text{Fe}_3\text{O}_4$  core with the silica shell has been carried out effectively. In addition, the FT-IR spectra of the recovered catalyst after being used six times are illustrated in Fig. 1d. It is worth noting that the acquired data represented no significant difference between the FT-IR spectra of as-prepared and that of the recovered nanocatalyst confirming the stability of the nanocatalyst under the reaction conditions.

In order to acquire information about the structural properties and crystallinity of the horsetail ash as well as that of encapsulated magnetite nanoparticles ( $\text{Fe}_3\text{O}_4\text{@HA}$ ), X-ray diffraction (XRD) analysis was performed and the comparative X-ray patterns were observed as shown in Fig. 2a, b. The characteristic small and sharp peak (at  $2\theta$  equal to  $22^\circ$  angle) was found in the XRD pattern of horsetail ash which could be attributed to the silica that is in  $\alpha$ -quartz phase (Fig. 2a). Powder XRD analysis of magnetic horsetail ash (Fig. 2b) shows six peaks at  $2\theta$  values =  $30.1^\circ$ ,  $35.4^\circ$ ,  $43.1^\circ$ ,  $53.4^\circ$ ,  $57^\circ$  and  $62.6^\circ$  which correspond to the (220), (311), (400), (422), (511) and (440) reflections were in good agreement with the standard pattern for crystalline magnetite with cubic structure as evidenced by the database of magnetite in the Joint Committee on Powder Diffraction Standards [JCPDS] (JCPDS card: 19–629) [50], revealing a high phase purity of magnetite. It is worth noting that the new peak with low intensity at  $2\theta = 22$  which was observed in Fig. 2b could be attributed to the characteristic peak of horsetail ash. This evidence indicates that the coating process did not result in the phase change of  $\text{Fe}_3\text{O}_4$  nanoparticles and corroborates the fact that the silica coating strategy is indeed successful in generating a protective silane shell around the magnetic core. Besides, the average crystalline size of  $\text{Fe}_3\text{O}_4\text{@HA}$  NPs which was calculated using Debye–Scherrer equation [51] is estimated to be 20 nm.

As shown in Fig. 3, the morphology and size distribution of  $\text{Fe}_3\text{O}_4\text{@HA}$  were calculated utilizing transmission electron microscopy (TEM). It can be

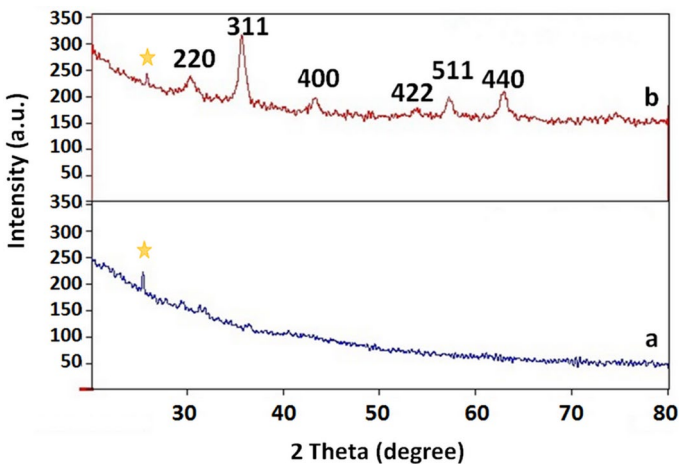
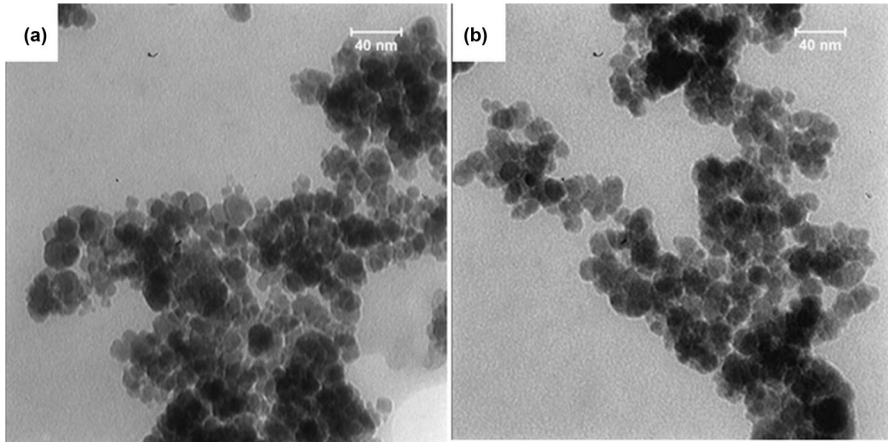


Fig. 2 XRD patterns of (a) Horsetail ash and (b)  $\text{Fe}_3\text{O}_4\text{@HA}$



**Fig. 3** TEM images of (a)  $\text{Fe}_3\text{O}_4@HA$  and (b) 6th reused  $\text{Fe}_3\text{O}_4@HA$

simply inferred from the TEM image of fresh  $\text{Fe}_3\text{O}_4@HA$  that the most prepared nanoparticles are spherical in shape (Fig. 3a). It also indicated the presence of prominent layers encapsulating the  $\text{Fe}_3\text{O}_4$ -NPs which proves the fact that the synthesized MNPs have core-shell structure. Based on distribution histogram of  $\text{Fe}_3\text{O}_4@HA$  (Fig. 4), the particle sizes of  $\text{Fe}_3\text{O}_4@HA$  in irregular geometric shape were found to be about 8–33 nm and the average diameter of nanoparticles was estimated to be 20 nm validating the results deduced from the XRD. Furthermore, the TEM image of  $\text{Fe}_3\text{O}_4@HA$  catalyst after being used six times, as shown in Fig. 3b indicated no obvious changes in the morphology structure of the catalyst even after experiencing six recoveries.

Scanning electron microscopy (SEM) images were recorded so as to analyze the morphology of the as-synthesized nanocatalyst. The SEM images of  $\text{Fe}_3\text{O}_4@HA$  which are presented in Fig. 5 indicate that nanoparticles are well dispersed

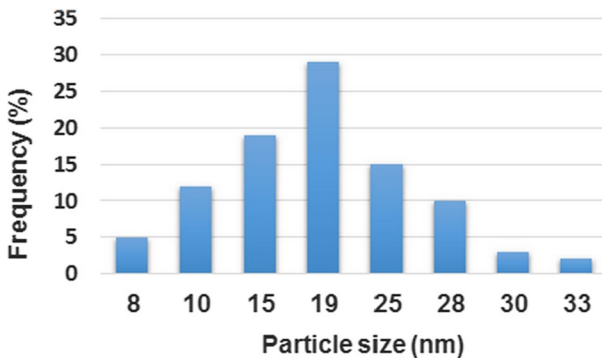


**Fig. 4** Particle size distribution histogram of  $\text{Fe}_3\text{O}_4@HA$

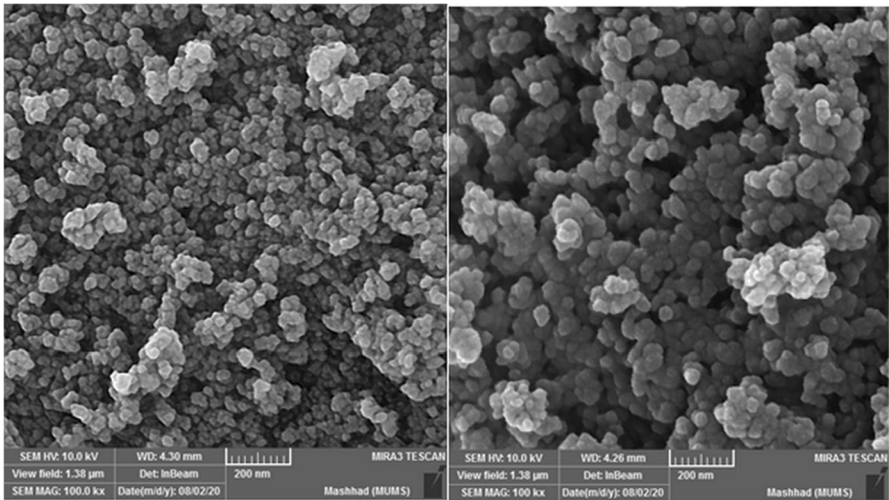


**Fig. 5** SEM images of  $\text{Fe}_3\text{O}_4\text{@HA}$

and they also demonstrate a regularly spherical morphology structure of nanometer-sized particles with an average diameter of 21 nm.

Additionally, the energy-dispersive X-ray (EDX) analysis was applied to calculate the elemental composition of the  $\text{Fe}_3\text{O}_4\text{@HA}$  MNPs. The EDX spectral pattern presented in Fig. 6, strongly demonstrates the chemical characterization of the typical catalyst sample with peaks for the O, Ca, Si, and Fe elements, verifying the construction and good distribution of  $\text{Fe}_3\text{O}_4\text{@HA}$  nanoparticles. Apart from that, the obtained results affirm the effective and successful grafting of horsetail ash onto the surface of  $\text{Fe}_3\text{O}_4$ . Also, it should be noted that no impurity elements were identified in the nanocatalyst structure.

A vibrating sample magnetometer (VSM) was implemented with the purpose of analyzing the magnetic properties of  $\text{Fe}_3\text{O}_4\text{@HA}$  nanoparticles at room temperature. In the VSM magnetization curve of  $\text{Fe}_3\text{O}_4\text{@HA}$  nanoparticles, no hysteresis

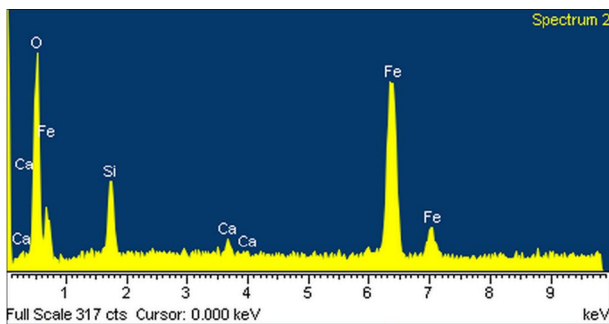


**Fig. 6** EDX analysis of  $\text{Fe}_3\text{O}_4\text{@HA}$

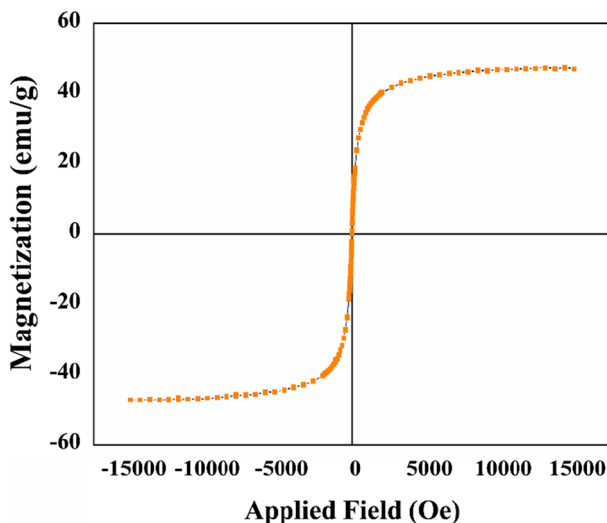


Fig. 7 The magnetization curve of  $\text{Fe}_3\text{O}_4$ @HA nanoparticles

was detected, and the remanence and coercivity are inconsequential and negligible, signifying the superparamagnetism of this nanomaterial (Fig. 7) [44, 52]. The saturation magnetization value of  $\text{Fe}_3\text{O}_4$ @HA was about  $47 \text{ emu g}^{-1}$  displaying that the magnetic sensitivity of the prepared catalyst is strong enough to be simply recycled from the reaction mixture by an external magnetic field which is substantial for both magnetic separation and reusability of the magnetic catalyst. Therefore, it could have promising applications as a renewable catalyst.

### Catalytic study

After  $\text{Fe}_3\text{O}_4$ @HA was characterized as a novel nano magnetic catalyst, we tried to investigate its catalytic effectiveness and productivity towards the synthesis of 2,4,5-trisubstituted imidazoles. For the purpose of achieving this objective, in the initial stage, a model reaction was selected upon the reaction of benzil (1 mmol), ammonium acetate as nitrogen source (2 mmol) and benzaldehyde (1 mmol) and following that, the role of various efficient parameters including the amount of catalyst, reaction temperature, reaction time, type of solvent system as well as solvent-free conditions was assessed in order to obtain the best outcomes regarding yield and reaction time. The findings of this optimization process are reported in Table 1. During the initial phase, the model reaction was investigated in several solvents such as  $\text{H}_2\text{O}$ , EtOH, MeCN, toluene and also solvent-free conditions in the presence of 0.01 g of the catalyst with the aim of choosing the reaction media. The product was obtained in 99, 75, 65, 55 and 25% yields, respectively (Table 1, entries 2–6). As a result,  $\text{H}_2\text{O}$  was found to be the most effective solvent for this reaction due to the fact that other solvents did not generate satisfactory results in comparison to it. Then the model reaction was tested in the presence of various

**Table 1** Optimization of various reaction parameters for the synthesis of 2,4,5 Triphenyl-1H-imidazole (4a<sup>a</sup>)

Entry	Catalyst (g)	Solvent	T (°C)	Time (min)	Conversion <sup>b</sup> %
1	–	–	100	110	< 10
2	Fe <sub>3</sub> O <sub>4</sub> @HA (0.01)	H <sub>2</sub> O	25	3	99
3	Fe <sub>3</sub> O <sub>4</sub> @HA (0.01)	EtOH	25	20	75
4	Fe <sub>3</sub> O <sub>4</sub> @HA (0.01)	MeCN	25	20	65
5	Fe <sub>3</sub> O <sub>4</sub> @HA (0.01)	Toluene	25	45	55
6	Fe <sub>3</sub> O <sub>4</sub> @HA (0.01)	–	25	80	25
7	Fe <sub>3</sub> O <sub>4</sub> @HA (0.005)	H <sub>2</sub> O	25	35	65
8	Fe <sub>3</sub> O <sub>4</sub> @HA (0.04)	H <sub>2</sub> O	25	3	99
9	Fe <sub>3</sub> O <sub>4</sub> @HA (0.01)	H <sub>2</sub> O	70	3	99
10	Horsetail ash (0.01)	H <sub>2</sub> O	25	12	87
11	Fe <sub>3</sub> O <sub>4</sub> (0.01)	H <sub>2</sub> O	25	100	45

<sup>a</sup>Reaction condition: benzil (1 mmol), benzaldehyde (1 mmol), ammonium acetate (2 mmol) and solvent (3 mL). <sup>b</sup>Isolated yield

amounts of the catalyst in H<sub>2</sub>O as solvent in order to determine the effect of the catalyst amount. Based on data displayed in Table 1, the reaction yield increased when the amount of the catalyst enhanced from 0.005 to 0.01 g and the best result was attained in the presence of 0.01 g of the catalyst. Moreover, reducing the amount of catalyst led to a decrease in the yield of the product (Table 1, entry 7). Notably, further increase in the amount of catalyst had no impacts on the yield and the reaction time (Table 1, entry 8) and also, no product was detected in the absence of the catalyst even after prolonged reaction time (Table 1, entry 1). At a later stage, the effect of reaction temperature was analyzed and the best result was achieved at 25 °C. By increasing the temperature from 25 to 70 °C, no significant rise in the yield was observed (Table 1, entry 9). The obtained results revealed that the best outcomes were acquired when 0.01 g of catalyst was utilized at room temperature in an aqueous medium (Table 1, entry 2). Moreover, horsetail ash and Fe<sub>3</sub>O<sub>4</sub> were separately used as catalysts in the model reaction under the same optimized conditions, in order to evaluate the impact of the nanocatalyst species on the reaction progress (Table 1, entries 10, 11). The catalytic performances of Fe<sub>3</sub>O<sub>4</sub> as catalyst were examined in model reaction and the obtained results revealed that Fe<sub>3</sub>O<sub>4</sub> based on having Lewis acidic properties could produce the product in trace amounts (Table 1, entry 11). According to the analyses performed on the horsetail ash which were fully investigated in our previous study, the horsetail ash was found to act as an acid catalyst itself whose catalytic features have been proved as Lewis acid. Consequently, further analyses of the received data indicated that when horsetail ash was applied separately as a catalyst in model reaction in the current research, the reaction was relatively good which yield to a higher product. All things considered; however, the catalytic activity of Fe<sub>3</sub>O<sub>4</sub>@HA was significantly higher leading to better outcomes. We attribute the obtained results to several factors including the conversion of horsetail ash to

nanomagnetic counterpart as well as the presence of Fe together with other metals existing in horsetail ash which have increased the catalytic activity of  $\text{Fe}_3\text{O}_4@$ HA.

Subsequently, with the optimal reaction conditions in hand, to investigate the efficiency and applicability of  $\text{Fe}_3\text{O}_4@$ HA as a magnetic nanocatalyst in the preparation of 2,4,5-trisubstituted imidazole derivatives, benzil **1** were treated with various aryl aldehydes **2** and ammonium acetate **3** in water (3 mL) at room temperature, to gain the corresponding products with good yields and short reaction times (Table 2, entries 1–16). Interestingly, the required imidazole products were achieved in excellent yields for both electron-rich and electron-poor aromatic aldehydes. Heteroaromatic aldehydes such as thiophene-2-carboxaldehyde and 1-naphthaldehyde also provided the corresponding products in high yields. The characterization of all the synthesized 2,4,5-trisubstituted imidazoles has been carried out through melting points and spectroscopic techniques such as FT-IR,  $^1\text{H}$  NMR and  $^{13}\text{C}$  NMR.

Eventually, the effectiveness of our presented protocol was investigated carefully in a comparative manner with some methods having been formerly reported for the synthesis of desired molecules. Considering the data reported in Table 3, a high competitive potential of the catalytic system described in the current paper compared with other previously reported systems was observed.

Following the patterns provided in the previous reports [40, 67] and in regard to our findings, a simple and satisfying mechanism for the synthesis of 2,4,5-trisubstituted imidazoles was proposed in Scheme 3. Initially, the reaction was considered to begin by an in situ generated ammonia from ammonium acetate. Meanwhile, the carbonyl groups of aldehyde [A] and benzil [B] were activated by  $\text{Fe}_3\text{O}_4@$ HA to provide intermediates [C] and [D], respectively. At a later stage, imine intermediates [E] and [F] were generated by nucleophilic addition of ammonia to activated aldehyde [C] and activated benzil [D], respectively. Then after, imine intermediate [E], condensed with the carbonyl group of [F] to produce carbocation [G]. Carbocation [G], right after the attack of the nitrogen atom of imine to the carbon atom of the iminium-positive center, supplies the cyclization with dehydration to form *iso*-imidazole [H], which successively rearranges the trisubstituted imidazoles by a [1, 5]-*H* shift.

Due to the fact that the reusability and easy recovery are among the most desirable and appealing characteristics of nanomagnetic catalysts, throughout our study, we focused on the reusability feature of  $\text{Fe}_3\text{O}_4@$ HA that is actually required and necessary for industrial applications. As a result, the reutilization trait of  $\text{Fe}_3\text{O}_4@$ HA as a nanocatalyst was examined in the model reaction (Fig. 8). Following the completion of the reaction, in order to separate nanocatalyst, hot ethanol was added to the reaction mixture. Then, the magnetic catalyst was readily isolated applying an external magnet, washed with ethanol and finally weighed for the further use under the same reaction conditions. As reflected in Fig. 8, it should be noted that after the catalyst was reused for six times in the same reaction and under the identical conditions, only an insignificant diminish in the yield of product was observed, indicating that the recovered catalyst after being used for six runs had no obvious change in structure as well as morphology, referring to the FT-IR spectra and TEM images in comparison with the fresh one.

**Table 2** Synthesis of 2,4,5-trisubstituted imidazole derivatives catalyzed by  $\text{Fe}_3\text{O}_4\text{@HA}^a$ 

$\text{Ph-CO-CO-Ph} + \text{Ar-CHO} + 2 \text{NH}_4\text{OAc} \xrightarrow[\text{H}_2\text{O (3mL), R.T.}]{\text{Fe}_3\text{O}_4\text{@HA (0.01 g)}} \text{Ph-C}_2\text{N(Ar)-C}_2\text{Ph}$

Entry	Aldehyde	Product	Time (min)	Yield <sup>b</sup> (%)	M.P. °C (Lit. <sup>Ref.</sup> )
1		 (4a)	3	99	274–275 (275–276 [53])
2		 (4b)	5	96	261–263 (262–264 [54])
3		 (4c)	7	97	191–193 (190–192 [53])
4		 (4d)	6	99	233–234 (232–233 [55])
5		 (4e)	10	95	267–269 (267–270 [56])
6		 (4f)	9	93	231–233 (230–233 [57])
7		 (4g)	10	91	296–298 (298–299 [58])
8		 (4h)	20	92	229–231 (232–233 [59])

Table 2 (continued)

Entry	Aldehyde	Product	Time (min)	Yield <sup>b</sup> (%)	M.P. °C (Lit. <sup>Ref.</sup> )
9		 (4i)	25	93	257–259 (258–260 [31])
10		 (4j)	10	94	205–207 (204–207 [60])
11		 (4 k)	12	98	261–263 (260–262 [54])
12		 (4 l)	15	95	230–232 (232–233 [61])
13		 (4 m)	8	92	229–231 (228–231 [57])
14		 (4n)	12	87	255–257 (256–258 [62])
15		 (4o)	20	90	295–297 (297 [27])
16		 (4p)	15	91	261–263 (260–262 [60])

<sup>a</sup>Reaction condition: benzil (1 mmol), aromatic aldehydes (1 mmol) and ammonium acetate (2 mmol) in the presence of 10 mg of Fe<sub>3</sub>O<sub>4</sub>@HA in 3 mL H<sub>2</sub>O at room temperature. <sup>b</sup>Isolated yield

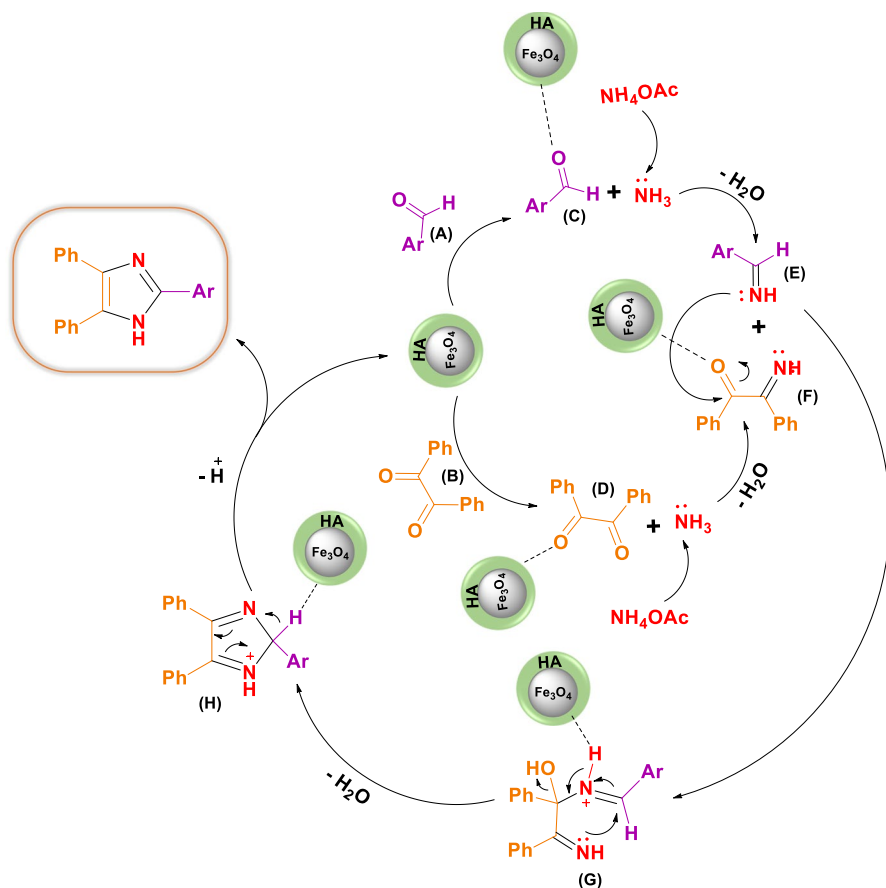
**Table 3** Comparison of catalytic activity of Fe<sub>3</sub>O<sub>4</sub>@HA with other catalysts previously reported in the literature for synthesis of compound 4a<sup>a</sup>

Entry	Catalyst	Reaction Condition	Time (min)	Yield <sup>b</sup> (%)	Ref
1	[Hbim]BF <sub>4</sub> <sup>c</sup> (4 mmol)	100 °C	60	95	[34]
2	Yb(OPf) <sub>3</sub> <sup>d</sup> (0.004 mmol)	HOAc, 2 mL; perfluorodecalin (C <sub>10</sub> F <sub>18</sub> , cis and trans-mixture), 1.5 mL, 80 °C	6 h	97	[41]
3	I <sub>2</sub> (5 mol%)	EtOH (2 mL), 75 °C	15	99	[29]
4	Sulphanilic acid (10 mol%)	EtOH / H <sub>2</sub> O (1:1 v/v; 20 mL), 80 °C	45	97	[63]
5	DABCO (0.7 mol %)	<i>t</i> -BuOH (10 mL), 60–65 °C	12 h	92	[38]
6	Scolecite (2 wt%)	EtOH (15 mL), reflux	35	96	[64]
7	-	Lactic acid (1 mL), 160 °C	180	90	[53]
8	-	Microwave irradiated at 150 W and 120 °C	5	93	[65]
9	-	EtOH, reflux	40	77	[66]
10	Fe <sub>3</sub> O <sub>4</sub> @g-C <sub>3</sub> N <sub>4</sub> <sup>e</sup> (20 mg)	EtOH (1 mL), 78 °C	2 h	95	[67]
11	BO <sub>3</sub> H <sub>3</sub> <sup>f</sup> (5 mol%)	EtOH / H <sub>2</sub> O (5:5 mL), Ultrasonication, r.t	30	98	[62]
12	[P <sub>4</sub> -VP]-Fe <sub>3</sub> O <sub>4</sub> <sup>g</sup> (100 mg)	100 °C	35	98	[54]
13	Fe <sub>3</sub> O <sub>4</sub> (5 mol%)	EtOH (10 mL), Ultrasonication, r.t	25	96	[40]
14	(NBS) <sup>h</sup> (15 mol%)	120 °C	50	89	[61]
15	Silica sulfuric acid (0.5 g)	water (30 ml), reflux	4 h	73	[68]
16	Al-MCM-41 (10 mg)	120 °C	45	91	[69]
17	KH <sub>2</sub> PO <sub>4</sub> <sup>i</sup> (5 mol%)	EtOH, reflux	40	93	[70]
18	Fe <sub>3</sub> O <sub>4</sub> @HA	H <sub>2</sub> O (3 mL), r.t	3	99	This Work

<sup>a</sup>Reaction condition: benzil (1 mmol), benzaldehyde (1 mmol) and ammonium acetate (2 mmol). <sup>b</sup>Isolated yield. <sup>c</sup>1-Butyl imidazolium tetrafluoroborate. <sup>d</sup>Ytterbium perfluorooctanesulfonate. <sup>e</sup>Magnetic graphitic carbon nitride. <sup>f</sup>Boric acid. <sup>g</sup>Cross-linked poly(4-vinylpyridine) supported Fe<sub>3</sub>O<sub>4</sub> nanoparticles. <sup>h</sup>N-bromosuccinimide. <sup>i</sup>Potassium dihydrogen phosphate

## Conclusion

To conclude, this study aimed to prepare horsetail ash from the exposure of horsetail to a high temperature at 400 °C. Based on the data acquired from the analysis of horsetail ash, it can be concluded that it possess acidic properties which are due to the presence of metallic ions in it, indicating that it could act as a potential lewis acid catalyst whose catalytic activity was completely examined and investigated in our earlier research. In the present work, it is highly recommended that the horsetail ash could be used as a natural silica resource having mesoporous structure. Accordingly, studies have been carried out to analyze the practical applications of horsetail ash as good support for the synthesis of magnetic horsetail ash and Fe<sub>3</sub>O<sub>4</sub>@HA as a magnetically heterogeneous solid acid nanocatalyst was prepared which was subsequently fully characterized by various analytical methods. This green and



**Scheme 3** Proposed mechanistic pathway for the preparation of 2,4,5-trisubstituted imidazole derivatives in the presence of  $\text{Fe}_3\text{O}_4@HA$

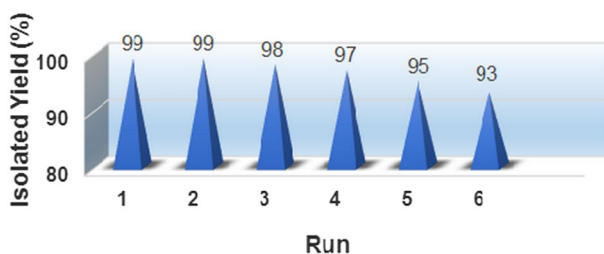


**Fig. 8** Synthesis of 2,4,5-Triphenyl-1H-imidazole (4a) in the presence of reused  $\text{Fe}_3\text{O}_4@HA$

new synthesized magnetic nanocatalyst was applied for the one-pot synthesis of 2,4,5-trisubstituted imidazole derivatives. The significant advantages of this methodology are characterized as excellent activity and stability, simple and effective

separation utilizing an appropriate external magnet resulting in minimizing the loss of catalyst during separation and its reusability for several times with no great loss of activity which make the present synthetic methodology more convenient and environmentally friendly in nature.

**Supplementary Information** The online version contains supplementary material available at <https://doi.org/10.1007/s11164-021-04420-y>.

**Acknowledgements** We are thankful to Ferdowsi University of Mashhad Research Council for financial support to this work (Grant no. p/3/45801).

**Declarations**

**Conflict of interest** The authors declare that they have no conflict of interest.

## References

1. P.T. Anastas, M.M. Kirchoff, *Acc. Chem. Res.* **35**, 686 (2002)
2. T. Cheng, D. Zhang, H. Li, G. Liu, *Green Chem.* **16**, 3401 (2014)
3. V. Polshettiwar, R.S. Varma, *Chem. Soc. Rev.* **37**, 1546 (2008)
4. M. Poliakoff, J.M. Fitzpatrick, T.R. Farren, P.T. Anastas, *Science* **297**, 807 (2002)
5. M. Esmailpour, J. Javidi, F. Nowroozi Dodeji, M. Mokhtari Abarghoui, *Transit. Met. Chem.* **39**, 797 (2014)
6. C. Sanjai, S. Kothan, P. Gonil, S. Saesoo, W. Sajomsang, *Carbohydr. Polym.* **104**, 231 (2014)
7. J.M. Montenegro, V. Grazu, A. Sukhanova, S. Agarwal, J.M. de la Fuente, I. Nabiev, A. Greiner, W.J. Parak, *Adv. Drug Deliv. Rev.* **65**, 677 (2013)
8. B. Karimi, F. Mansouri, H.M. Mirzaei, *ChemCatChem* **7**, 1736 (2015)
9. Y. Zhu, L.P. Stubbs, F. Ho, R. Liu, C.P. Ship, J.A. Maguire, N.S. Hosmane, *ChemCatChem* **2**, 365 (2010)
10. S.I. Stoeva, F. Huo, J.S. Lee, C.A. Mirkin, *J. Am. Chem. Soc.* **127**, 15362 (2005)
11. M.A. Correa Duarte, M. Grzelczak, V. Salgueiriño Maceira, M. Giersig, L.M. Liz Marzán, M. Farle, K. Sieradzki, R. Diaz, *J. Phys. Chem. B* **109**, 19060 (2005)
12. A. Mobaraki, B. Movassagh, B. Karimi, *A.C.S. Comb. Sci.* **16**, 352 (2014)
13. N. Hosseini Mohtasham, M. Gholizadeh, *J. Iran. Chem. Soc.* **17**, 397 (2020)
14. F. Bellina, S. Caution, R. Rossi, *Tetrahedron* **63**, 4571 (2007)
15. R.W. Brimblecombe, W.A.M. Duncan, G.J. Durant, J.C. Emmett, C.R. Ganellin, M.E. Parsons, *J. Int. Med. Res.* **3**, 86 (1975)
16. S. Dutta, G. Mariappan, S. Roy, M. Verma, *Indian Drugs* **46**, 50 (2009)
17. S.A. Laufer, W. Zimmermann, K.J. Ruff, *J. Med. Chem.* **47**, 6311 (2004)
18. P. Magdolen, A. Vasella, *Helv. Chim. Acta* **88**, 2454 (2005)
19. L. Navidpour, H. Shadnia, H. Shafaroodi, M. Amini, A.R. Dehpour, A. Shafiee, *Bioorg. Med. Chem.* **15**, 1976 (2007)
20. Ü. Uçucu, N.G. Karaburun, İ. İşikdağ, *Farmaco* **56**, 285 (2001)
21. J.R. Coura, S.L. De Castro, *Mem. Inst. Oswaldo Cruz* **97**, 3 (2002)
22. J. Dupont, R.F. de Souza, P.A.Z. Suarez, *Chem. Rev.* **102**, 3667 (2002)
23. S.J. Nara, P.U. Naik, J.R. Harjani, M.M. Salunkhe, *Indian J. Chem. B* **45B**, 2257 (2006)
24. S. Chowdhury, R.S. Mohan, J.L. Scott, *Tetrahedron* **63**, 2363 (2007)
25. D. Bourissou, O. Guerret, F.P. Gabbai, G. Bertrand, *Chem. Rev.* **100**, 39 (2000)
26. P.L. Arnold, S.T. Liddle, *Chem. Commun.* 3959 (2006)
27. M.V. Chary, N.C. Keerthysri, S.V.N. Vupallapati, N. Lingaiah, S. Kantevari, *Catal. Commun.* **9**, 2013 (2008)
28. S.D. Sharma, P. Hazarika, D. Konwar, *Tetrahedron Lett.* **49**, 2216 (2008)
29. M. Kidwai, P. Mothra, V. Bansal, R.K. Somvanshi, A.S. Ethayathulla, S. Dey, T.P. Singh, *J. Mol. Catal. A Chem.* **265**, 177 (2007)

30. H.A. Oskooie, Z. Alimohammadi, M.M. Heravi, *Heteroat. Chem.* **17**, 699 (2006)
31. S. Samai, G.C. Nandi, P. Singh, M.S. Singh, *Tetrahedron* **65**, 10155 (2009)
32. G.V.M. Sharma, Y. Jyothi, P.S. Lakshmi, *Synth. Commun.* **36**, 2991 (2006)
33. N.V. Shitole, K.F. Shelke, S.S. Sonar, S.A. Sadaphal, B.B. Shingate, M.S. Shingare, *Bull. Korean Chem. Soc.* **30**, 1963 (2009)
34. S.A. Siddiqui, U.C. Narkhede, S.S. Palimkar, T. Daniel, R.J. Lahoti, K.V. Srinivasan, *Tetrahedron* **61**, 3539 (2005)
35. A. Gharib, B. Hashemipour Khorasani, M. Jahangir, M. Roshani, L. Bakhtiari, S. Mohadeszadeh, *Bulg. Chem. Commun.* **46**, 165 (2014)
36. Y.R. Girish, K.S. Sharath Kumar, K.N. Thimmaiah, K.S. Rangappa, S. Shashikanth, *RSC Adv.* **5**, 75533 (2015)
37. M. Hajjami, A. Ghorbani Choghamarani, Z. Yousofvand, M. Norouzi, *J. Chem. Sci.* **127**, 1221 (2015)
38. S.N. Murthy, B. Madhav, Y.V.D. Nageswar, *Tetrahedron Lett.* **51**, 5252 (2010)
39. J. Safari, S. Gandomi Ravandi, Z. Akbari, *Iran. J. Catal.* **3**, 33 (2013)
40. J. Safari, Z. Zarnegar, *Iran. J. Catal.* **2**, 121 (2012)
41. M.G. Shen, C. Cai, W.B. Yi, *J. Fluor. Chem.* **129**, 541 (2008)
42. A. Teimouri, A. Najafi Chermahini, *J. Mol. Catal. A Chem.* **346**, 39 (2011)
43. H. Zang, Q. Su, Y. Mo, B.W. Cheng, S. Jun, *Ultrason. Sonochem.* **17**, 749 (2010)
44. F. Adam, K. Kandasamy, S. Balakrishnan, *J. Colloid Interface Sci.* **304**, 137 (2006)
45. B.M. Cherian, L.A. Pothan, T. Nguyen Chung, G. Mennig, M. Kottaisamy, S. Thomas, *J. Agric. Food Chem.* **56**, 5617 (2008)
46. X.F. Sun, F. Xu, R.C. Sun, P. Fowler, M.S. Baird, *Carbohydr. Res.* **340**, 97 (2005)
47. E. Kolvari, N. Koukabi, M.M. Hosseini, *J. Mol. Catal. A Chem.* **397**, 68 (2015)
48. D.V. Quang, J.E. Lee, J.K. Kim, Y.N. Kim, G.N. Shao, H.T. Kim, *Powder Technol.* **235**, 221 (2013)
49. J. Sun, G. Yu, L. Liu, Z. Li, Q. Kan, Q. Huo, J. Guan, *Catal. Sci. Technol.* **4**, 1246 (2014)
50. M. Esmailpour, A.R. Sardarian, J. Javidi, *Appl. Catal. A Gen.* **445–446**, 359 (2012)
51. E.M.M. Ibrahim, A.M. Abu Dief, A. Elshafaie, A.M. Ahmed, *Mater. Chem. Phys.* **192**, 41 (2017)
52. L. Zhang, W.F. Dong, H.B. Sun, *Nanoscale* **5**, 7664 (2013)
53. J. Sonar, S. Pardeshi, S. Dokhe, R. Pawar, K. Kharat, A. Zine, B. Matsagar, K. Wu, S. Thore, S.N. Appl. Sci. **1**, 1045 (2019)
54. Z. Hamidi, M.A. Karimi Zarchi, *Res. Chem. Intermed.* **44**, 6995 (2018)
55. M. Alikarami, M. Amozad, *Bull. Chem. Soc. Ethiop.* **31**, 177 (2017)
56. E. Kanaani, M. Nasr Esfahani, *J. Chin. Chem. Soc.* **66**, 119 (2019)
57. J. Safari, S. Dehghan Khalili, S.H. Banitaba, *J. Chem. Sci.* **122**, 437 (2010)
58. N. Azizi, N. Dado, A. Khajeh Amiri, *Can. J. Chem.* **90**, 195 (2012)
59. H. Aghahosseini, A. Ramazani, K. Ślepokura, T. Lis, *J. Coll. Interf. Sci.* **511**, 222 (2018)
60. H.R. Shaterian, M. Ranjbar, *J. Mol. Liq.* **160**, 40 (2011)
61. B. Maleki, S. Sedigh Ashrafi, *J. Mex. Chem. Soc.* **58**, 76 (2014)
62. K.F. Shelke, S. Sapkal, S. Sonal, B.R. Madje, B.B. Shingate, M.S. Shingare, *Bull. Korean Chem. Soc.* **30**, 1057 (2009)
63. A.F. Mohammed, N.D. kokare, J.N. Sangshetti, D.B. Shinde, *J. Korean Chem. Soc.* **51**, 418 (2007)
64. L.S. Gadekar, S.R. Mane, S.S. Katkar, B.R. Arbad, M.K. Lande, *Cent. Eur. J. Chem.* **7**, 550 (2009)
65. J.F. Zhou, G.X. Gong, X.J. Sun, Y.L. Zhu, *Synth. Commun.* **40**, 1134 (2010)
66. R. Tayebee, A. Gohari, *Eurasian. Chem. Commun.* **2**, 581 (2020)
67. T. Soleymani Ahoovie, N. Azizi, I. Yavari, M. Mahmoudi Hashemi, *J. Iran. Chem. Soc.* **15**, 855 (2018)
68. A. Shaabani, A. Rahmati, *J. Mol. Catal. A Chem.* **249**, 246 (2006)
69. A. Olyaei, Z. Derikvand, F. Noruzian, M. Sadeghpour, *Quarter. J. Iran Chem. Commun.* **4**, 337 (2016)
70. R.S. Joshi, P.G. Mandhane, M.U. Shaikh, R.P. Kale, C.H. Gill, *Chin. Chem. Lett.* **21**, 429 (2010)

**Publisher's Note** Springer Nature remains neutral with regard to jurisdictional claims in published maps and institutional affiliations.

## Authors and Affiliations

Nina Hosseini Mohtasham<sup>1</sup> · Mostafa Gholizadeh<sup>1</sup> 

✉ Mostafa Gholizadeh  
m\_gholizadeh@um.ac.ir

<sup>1</sup> Department of Chemistry, Faculty of Science, Ferdowsi University of Mashhad, Mashhad, Iran